International Journal of Nanomedicine

Dovepress
open access to scientific and medical research

Open Access Full Text Article

ORIGINAL RESEARCH

Antimicrobial and antibiofilm activity of biopolymer-Ni, Zn nanoparticle biocomposites synthesized using *R. mucilaginosa* UANL-001L exopolysaccharide as a capping agent

This article was published in the following Dove Press journal:
International Journal of Nanomedicine

Javier Alberto Garza-Cervantes[1,2]
C Enrique Escárcega-González[1–3]
E Díaz Barriga Castro[4]
G Mendiola-Garza[1,2]
Bruno Antonio Marichal-Cancino[3]
Mario Alberto López-Vázquez[3]
Jose Ruben Morones-Ramirez[1,2]

[1]Universidad Autónoma de Nuevo León, UANL, Facultad de Ciencias Químicas, San Nicolás de los Garza, NL 66451, México; [2]Centro de Investigación en Biotecnología y Nanotecnología, Facultad de Ciencias Químicas, Universidad Autónoma de Nuevo León, Parque de Investigación e Innovación Tecnológica, Apodaca 66629, Nuevo León, México; [3]Universidad Autónoma de Aguascalientes, Departamento de Fisiología y Farmacología, Centro de Ciencias Básicas, Aguascalientes, Mexico; [4]Centro de Investigación en Química Aplicada, Saltillo, Coahuila, México

Correspondence: Jose Ruben Morones-Ramirez
Universidad Autónoma de Nuevo León, UANL, Facultad de Ciencias Químicas, Av. Universidad s/n. CD. Universitaria, San Nicolás de los Garza 66451, NL, México
Tel +52 818 329 4000 Ext 3439
Email jose.moronesrmr@uanl.edu.mx; jose.moronesrmr@uanl.edu.mx

Introduction: Global increase in the consumption of antibiotics has induced selective stress on wild-type microorganisms, pushing them to adapt to conditions of higher antibiotic concentrations, and thus an increased variety of resistant bacterial strains have emerged. Metal nanoparticles synthesized by green methods have been studied and proposed as potential antimicrobial agents against both wild-type and antibiotic-resistant strains; in addition, exopolysaccharides have been used as capping agent of metal nanoparticles due to their biocompatibility, reducing biological risks in a wide variety of applications.

Purpose: In this work, we use an exopolysaccharide, from *Rhodotorula mucilaginosa* UANL-001L, an autochthonous strain from the Mexican northeast, as a capping agent in the synthesis of Zn, and Ni, nanoparticle biopolymer biocomposites.

Materials and methods: To physically and chemically characterize the synthesized biocomposites, FT-IR, UV-Vs, TEM, SAED and EDS analysis were carried out. Antimicrobial and antibiofilm biological activity were tested for the biocomposites against two resistant clinical strains, a Gram-positive *Staphylococcus aureus*, and a Gram-negative *Pseudomonas aeruginosa*. Antimicrobial activity was determined using a microdilution assay whereas antibiofilm activity was analyzed through crystal violet staining.

Results: Biocomposites composed of exopolysaccharide capped Zn and Ni metal nanoparticles were synthesized through a green synthesis methodology. The average size of the Zn and Ni nanoparticles ranged between 8 and 26 nm, respectively. The Ni-EPS biocomposites showed antimicrobial and antibiofilm activity against resistant strains of *Staphylococcus aureus* and *Pseudomonas aeruginosa* at 3 and 2 mg/mL, respectively. Moreover, Zn-EPS biocomposites showed antimicrobial activity against resistant *Staphylococcus aureus* at 1 mg/mL. Both biocomposites showed no toxicity, as renal function showed no differences between treatments and control in the in vivo assays with male rats tests in this study at a concentration of 24 mg/kg of body weight.

Conclusion: The exopolysaccharide produced by *Rhodotorula mucilaginosa* UANL-001L is an excellent candidate as a capping agent in the synthesis of biopolymer-metal nanoparticle biocomposites. Both Ni and Zn-EPS biocomposites demonstrate to be potential contenders as novel antimicrobial agents against both Gram-negative and Gram-positive clinically relevant resistant bacterial strains. Moreover, Ni-EPS biocomposites also showed antibiofilm activity, which makes them an interesting material to be used in different applications to counterattack global health problems due to the emergence of resistant microorganisms.

Keywords: nickel, zinc, nanoparticles, antibiofilm activity, exopolysaccharide capping agent

submit your manuscript | www.dovepress.com
DovePress
http://doi.org/10.2147/IJN.S196470

Introduction

Since the discovery of penicillin, during the 60 years of the antibiotic golden era, pharmaceutical companies fueled large-scale production of a wide variety of biologically active compounds.[1] The increased and inappropriate global use of these antibiotics has induced a selective stress on microorganisms, pushing them to adapt to higher concentrations of antibiotics and leading to the emergence of resistant bacterial strains such as the ESKAPE pathogens,[2] a group of very difficult to treat microorganisms that include: the *Enterococcus, Staphylococcus, Klebsiella, Acinetobacter, Pseudomonas* and *Enterobacter* resistant strains. This problem has worsened within the last decade due to faster pathogenic bacteria adaptation and a decreased number of new antibiotics being produced down the pipeline.[3,4] Antibiotic-resistant *Staphylococcus aureus* and *Pseudomonas aeruginosa* are two pathogens with relevant clinical impact. Both strains have the ability to attach to surfaces and produce biofilms, which confers them up to 1,500 fold more resistance and tolerance to antimicrobial compounds and physical stress when compared to their planktonic state.[5–7] Infections, where biofilms are present, are very difficult to treat since they act as a constant infection source that periodically releases planktonic bacteria. Moreover, these biofilms can be found on wet, damp and even dry surfaces, representing a serious problem in medical devices related infections since the bacteria can widely spread in ortho-dental prosthetics, contact lenses, cardiovascular valves, urinary catheters, pacemakers and breast implants.[5,8] It has been estimated that biofilm producing bacterial strains are responsible for more than 65% of the nosocomial infections and up to 80% of occasional infections.[9] A challenging approach to biofilm eradication is the discovery or innovation of novel potent antibiofilm compounds. Recently, there has been a growing interest to explore the antibiofilm properties of exopolysaccharides (EPS) and glyco-compounds due to their biochemical structure and their biological applications.[10] Polysaccharides commonly found outside the cell are known as EPS and some of these compounds have been reported to display interesting features, such as a capacity to inhibit growth and biofilm production in some microorganisms.[11] This biological activity is due to the ability of EPS to modify biotic and abiotic surfaces, therefore decreasing the ability of microorganisms to attach onto different surfaces.[11–14] Therefore, EPS produced in different microorganisms propose a promising alternative as antibiofilm and antibiotics agents for the industrial and medical sector.

Transition metals species are among the most studied alternative antimicrobial agents.[15,16] Specifically, silver compounds have been widely used as antimicrobial agents since ancient times. Nonetheless, it is not the only transition metal that has been explored as an antimicrobial agent: zinc[17–20] and nickel[21,22] compounds have been shown to also exhibit antimicrobial activity. However, one of the main limitations to employ these compounds as therapeutic agents is their high toxicity to eukaryotic cells. To overcome the cytotoxicity drawbacks of using transition metals, proper combinatorial formulations with other antimicrobial agents have been proposed.[23,24] As an additional alternative to eliminate toxicity of transition metals in eukaryotes, the use of biopolymer-metal nanoparticle (NP) biocomposites has been proposed since there are reports where the toxicity can be reduced using this approach. These biocomposites are mostly produced through green synthesis methods, eliminating the use of toxic chemicals and allowing their use in pharmaceutical and biological applications.[25] Typical capping agents employed on NP synthesis are: long-chain hydrocarbons, polymers, block co-polymer and green capping agents. For instance, the usage of heteroatom-functionalized long-chain hydrocarbons has a significant contribution in the control of size and morphology monodispersity, but due to the complexity to remove these heteroatoms before their employment on industrial purposes, their implementation is economically unfavorable.[26] Recently, microbial EPS have been used in the synthesis of a variety of metallic NPs as capping agents,[27–31] since they are biocompatible, non-toxic and easily biodegradable. Using microbial EPS in the synthesis of biocomposites allows scalability and decreased production costs, time reduction in the synthesis and increased safety.[32–35]

In this work, we hypothesized that microbial EPS produced in *Rhodotorula mucilaginosa*, an autochthonous strain from the Mexican northeast, could act as a capping agent in the synthesis of biopolymer Zn and Ni NP biocomposites, as it has not been reported for EPS produced by this microorganism. We obtained Zn and Ni NPs that were characterized through UV-Vis spectrometry, FT-IR and TEM. The Zn and Ni NPs in the biocomposite had an average size of 8 and 26 nm, respectively. Ni-EPS

biocomposites were capable of inhibiting resistant strains of *Pseudomonas aeruginosa* (PaR) and *Staphylococcus aureus* (SaR) at 2 and 3 mg/mL, respectively. Zn-EPS biocomposites were capable of inhibiting resistant *Staphylococcus aureus* at 1 mg/mL. Furthermore, Ni-EPS biocomposites inhibited biofilm formation in up to 90% in both clinical strains at the inhibitory concentrations. Also, there was no toxicity effect, as renal function was similar in the control and the treatments, in the in vivo assays made with male rats tests in this study at a concentration of 24 mg/kg of body weight.

Materials and methods

EPS extraction from rhodotorula mucilaginosa culture

EPS was produced by inoculating with *R. mucilaginosa* 5 mL of Yeast Mold medium (YM) and incubated for 16 h at 30°C. From this overnight culture, 1 mL was transferred to 300 mL of fresh YM to incubate for 96 h at 30°C and 150 rpm. After the incubation time, the supernatant was recovered by centrifugation at 12000 rpm for 20 min at 4°C. The EPS was precipitated adding 3 volumes of absolute ethanol per volume of supernatant and stored at −20°C overnight. The precipitated EPS was centrifuged at 12000 rpm for 20 min at 4°C and washed three times with ethanol. The EPS samples were dried in a concentrator SpeedVac SPD2010, for a run time of 5 h at 5.1 torr, heating for 1 h at 45°C.

Synthesis of EPS-metal NPs

Metal NP-EPS biocomposites were synthesized by reducing zinc or nickel sulfate (Productos Químicos Monterrey, México) with ascorbic acid (Jalmek, México) in the presence of the microbial EPS which served as a capping agent in the synthesis. For the synthesis of the Zn-EPS biocomposites, a mixture of 100 mM $ZnSO_4$, 2 mg/mL of EPS and 10% w/v ascorbic acid was adjusted to pH 9 with NaOH (Jalmek, México) and heated in a boiling water bath for 30 min. For the synthesis of the Ni-EPS biocomposites, a mixture of 10 mM $NiSO_4$, 5 mg/mL of EPS and 4% w/v ascorbic acid was adjusted to pH 9 with NaOH and heated in a boiling water bath for 4 h. K_2SO_4 (Jalmek, México) was used to have a control mixture where no metal was included; this control was prepared to have the same concentration of EPS and ascorbic acid as in the Zn or Ni reaction. The synthesized solution was then added into three volumes of absolute ethanol and stored at −20°C for 1 h. Further, the mixture was centrifuged at 12000 rpm for 15 min at 4°C and washed three times with ethanol at 70%. The NPs were dried in a concentrator SPD2010 SpeedVac (ThermoFischer Scientific, USA) for a run time of 5 h at 5.1 torr, heating for 1 h at 45°C.

Material characterization

A Multiskan-GO (Thermo Scientific, USA) in the range of 200–800 nm was used to perform UV-Vis spectrophotometry and to identify the surface plasmon resonance (SPR) of the metal NPs within the biocomposites. An IRAfinity-1 (Shimadzu, Japan) was employed to perform Fourier transform-infrared spectroscopy (FTIR) analysis to characterize functional groups of the EPS and the synthesized NPs within the biocomposite. Morphological and structural characteristics of the Zn-EPS biocomposites were studied using transmission electron microscopy (TEM) and selected area electron diffraction (SAED) in a FEI-TITAN 80–300 microscope operated at an accelerating voltage of 300 kV. The specimen for these studies was prepared by depositing and evaporating a drop of the colloidal solution (1 mg/mL), previously dispersed by means of an ultrasonic cleaner (BRANSONIC, Branson 2510MT), onto lacey carbon-coated copper grids. The elements present in the samples were determined using an energy dispersive spectrometry analyzer (EDS) integrated in the TEM. In relation to the particle size, TEM images were used to measure the diameter of more than 100 NPs to estimate the size distribution of our NPs using the image processing software ImageJ (National Health Institute). A Nanotrac wave (Microtrac, USA) was used to determine zeta potential values of the synthesized NPs.

Bacterial growth inhibition by EPS capped NPs

Minimal inhibitory concentration (MIC) was assessed in 96-well plates (Costar-Corning) based on a modified methodology previously reported.[23] Stocks of Zn- and Ni-NPs were prepared at a final concentration of 8 mg/mL using LB adjusted to pH 7 with phosphate buffer 0.1 M (LB) as the vehicle. For each metal-EPS biocomposite, we added a bacteria inoculum and the necessary LB volume to each well to achieve different concentrations of the metal-EPS biocomposite; these concentrations varied between 4, 3, 2 and 1 mg/mL after the bacteria inoculum is added.

To inoculate each test well in the MIC assay, an overnight culture (20 h of culture incubated at 37°C – 150 rpm)

in LB for each strain, resistant *Pseudomonas aeruginosa (PaR)* and resistant *Staphylococcus aureus (SaR)*, were diluted 1:100 in fresh LB medium and incubated until it reached a critical optical density (OD_{600} of 0.2±0.02). Thereon, a 1:20 dilution was made with fresh LBb medium, and then 20 µL of this dilution was added to each test well to achieve a final concentration of 10^5 cells/mL, following incubation at 37°C and 150 rpm.

After 20 h of incubation at 37°C, the ODs of the control and the treated samples were measured. We next determined the MIC for each EPS-capped NP corresponded to the concentration at which no significant growth was observed (OD_{600}<0.05). All tests and their respective control samples were performed in triplicates.

Antibacterial mechanism of EPS-capped NPs

Antimicrobial mechanisms of the synthesized composites were explored by measuring the leakage of intracellular reducing sugars. Both bacterial strains were analyzed by this assay. For each compound, we added the necessary volume of biocomposite to achieve 3 mg/mL in every test well once the inoculum was added. To inoculate each test well, we proceeded as specified in the bacterial growth inhibition assay and incubated at 37°C and 150 rpm for 4 h.

After the incubation time, the plates were centrifuged at 3500 rpm for 15 min, and then 5 µL of supernatant were used to determine reducing sugars by Miller's method.[36]

Inhibition of biofilm formation by EPS-capped metal NPs

The antibiofilm assays were performed by exposing bacteria to different concentrations of the metal-EPS biocomposites in 96-well plates. Antibiofilm activity was analyzed by a crystal violet staining microtiter biofilm formation assay.[37] Different concentrations of the EPS-capped Zn and Ni NPs, and EPS alone were added to each well as follows: 1, 2, 3 and 4 mg/mL. A control culture without treatment was grown in the same plate. Each well was inoculated with a final concentration of 105 cells/mL, incubated at 37°C for 40 hrs under static conditions.

After the incubation time, the supernatant was removed, and each well was washed 3 times with ultrapure water. The plates were heat dried and each well was stained with 240 µL of crystal violet 0.1% for 20 min under static conditions. Next, the dye was removed, and each plate was washed 3 times with ultrapure water and heat dried. Biofilms were de-stained using an ethanol 99% solution for 30 min under static conditions. 100 µL of the ethanol/crystal violet were transferred to another plate and the optical density was measured at 590 nm. All tests, as well as the untreated control, were performed in triplicates.

In vivo toxicological study

Animals

Male adult Wistar rats (200–250 g) were used and maintained in stainless steel cages with a 12 h light/dark regime. All of the experimental animals were handled according to the Guiding Principles in the Use of Animals in Toxicology.

Experimental design

To test the safety of the Zn and Ni NPs, as well as the safety of EPS produced in this study, a renal toxicology study was performed in male Wistar rats. Briefly, after anesthetizing the animals with isoflurane, 4 groups of animals (control, EPS, Ni NPs and Zn NPs, with n=4 in all groups) were exposed to the metal-EPS biocomposite and the EPS alone by orally administrating 1 mL of the metal-EPS biocomposite or the EPS alone at concentrations of 6 mg/mL. For the case of the control group, 1 mL of the phosphate buffer 0.1 M was administered orally to the animals. The dosing regime was one administration of the buffer, NPs and EPS during each 24 h for 3 days. During all experiments, the rats were kept with food and water *ad libitum* and at room temperature (24±1°C). After 24 hrs of the third day of dosing, urine samples were obtained placing the rats in metabolic cages (3700M020; Tecniplast, Buguggiate (VA), Italy) where urine is collected in vessels attached to the metabolic cages. Blood samples were also obtained to finally sacrifice the experimental animals.

Biochemical tests

To analyze the renal function of the animals exposed to the NPs and EPS, urinary volume, urinary concentration of glucose,[38] proteins[39] and creatinine,[40,41] as well as blood plasma concentration of creatinine[40,41] was measured with their respective methods by means of UV-VIS spectrophotometer (DMS 80; Varian, Palo Alto, CA, USA).

Data analysis

To estimate the significance of the observed differences between the treatments employed, all collected data were

subjected to an analysis of variance (ANOVA) and Fisher's least significant difference (LSD) tests, using Microsoft Excel 2016.

Ethics approval and informed consent

Animal care and experimentation practices at the Universidad Autónoma de Aguascalientes are constantly evaluated by the Animal Care and Use Committee, adhering to the official Mexican Regulations (NOM-062-ZOO-1999). Mexican regulations are in strict accordance with the recommendations in the Guide for the Care and Use of Laboratory Animals of the NIH and the Weatherall Report of the USA to ensure compliance with established international regulations and guidelines. Experimental protocols were approved by the local Institutional Bioethical Committee. At the end of experiments, animals were sacrificed by using an excess of sodium pentobarbital anesthesia (40 mg/kg bw). Efforts were made to minimize suffering.

Results

Exopolysaccharide extracted from rhodotorula mucilaginosa UANL-001L

After incubating *R. mucilaginosa* cultures for 96 h at 30°C, EPS was produced with a yield of 413.9 mg/mL. The EPS was characterized by FTIR and as displayed in Figure 1 the peaks show a broad band at 3600–3200 cm^{-1}, 2900 cm^{-1}, 1650 cm^{-1}, 1420 cm^{-1}, 1350 cm^{-1} and various peaks around 1050–1250 cm^{-1}, as reported in the literature.[42]

Zn and Ni NPs synthesis and characterization

The metal-EPS biocomposites were produced in aqueous solution, adjusted with NaOH to pH 9, containing *R. mucilaginosa* EPS as capping agent and ascorbic acid as a reducing agent. The biocomposites were characterized using UV-Vis spectrophotometry and the spectra are shown in Figure 2. It can be observed that the maximum absorption is at 347 nm and 348 nm for Zn- and Ni-EPS biocomposites, respectively. EPS, Zn(II) and Ni(II) solutions at concentrations used in the synthesis, as well as reactions made without Zn(II) and Ni(II), are shown in Figure 2 as a comparison with the produced NPs. FTIR of the synthesized metal-EPS biocomposite was also performed and the results in Figure 1 show that no new peaks appear after the reaction to synthesize the capped NPs. The Zn-EPS biocomposite showed peaks at 3600–3200 cm^{-1} for O–H, 1600 cm^{-1} for C=O stretch, 1450–1400 cm^{-1} to C–H bending, 1300–1350 cm^{-1} to C–O stretch and 1050–1250 cm^{-1} to C–O–C of sugar

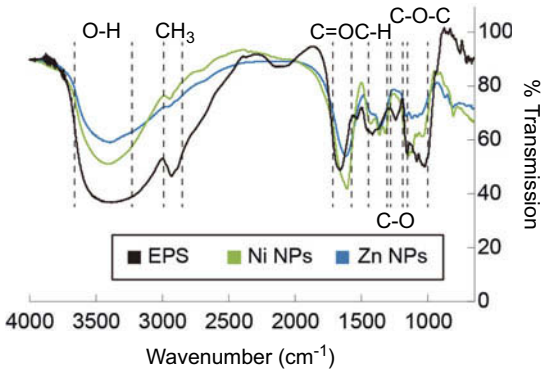

Figure 1 Comparison of FTIR spectra of EPS before and after metal reactions. Black line corresponds to EPS as used for the reactions. Blue line corresponds to EPS with the synthesized Zn nanoparticles. Green line corresponds to EPS with the synthesized Ni nanoparticles.
Abbreviations: FTIR, Fourier transform-infrared spectroscopy; EPS, exopoly saccharides.

derivates. NiNPs showed peaks at 3600–3200 cm^{-1} for O–H, 1600 cm^{-1} for C=O stretch, 1450–1400 cm^{-1} to C–H bending, 1300–1350 cm^{-1} to C–O stretch and 1020–1250 cm^{-1} for C–O–C in sugar derivates.

TEM images of the metal-EPS biocomposites demonstrate that, for the Zn-EPS biocomposite, there is a polymorphic arrangement without definite shape (Figure 3A). The ZnNPs have a diameter size that ranges from 4 to 11 nm with an average size of 8.32±1.99 nm. A SAED pattern of the Zn-EPS biocomposite presented bright rings and spots that are correlated to the [1,0,0], [0,0,2], [1,0,1], [1,1,0], [1,0,3], [2,0,0], [1,1,2], [2,0,1], [2,1,0], [3,0,0] and [2,1,3] planes of a hexagonal geometry in ZnO (Figure 3B). Further characterization of the EPS-capped ZnNPs by EDS analysis demonstrates the presence of Zn, C and O, thus confirming the presence of ZnNPs in

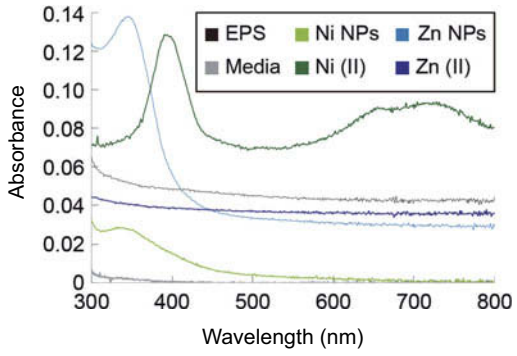

Figure 2 UV-Vis spectra of the EPS and the synthesized nanoparticles. Black line represents the EPS as used before reactions, light blue line represents the Zn nanoparticles synthesized, dark blue line represents the Zn(II) ions at concentration used in the synthesis reaction, the light green line represents the Ni nanoparticles synthesized, dark green line represents the Ni(II) ions at concentration used in the synthesis reaction and the gray line represents the sample media.
Abbreviation: EPS, exopolysaccharides.

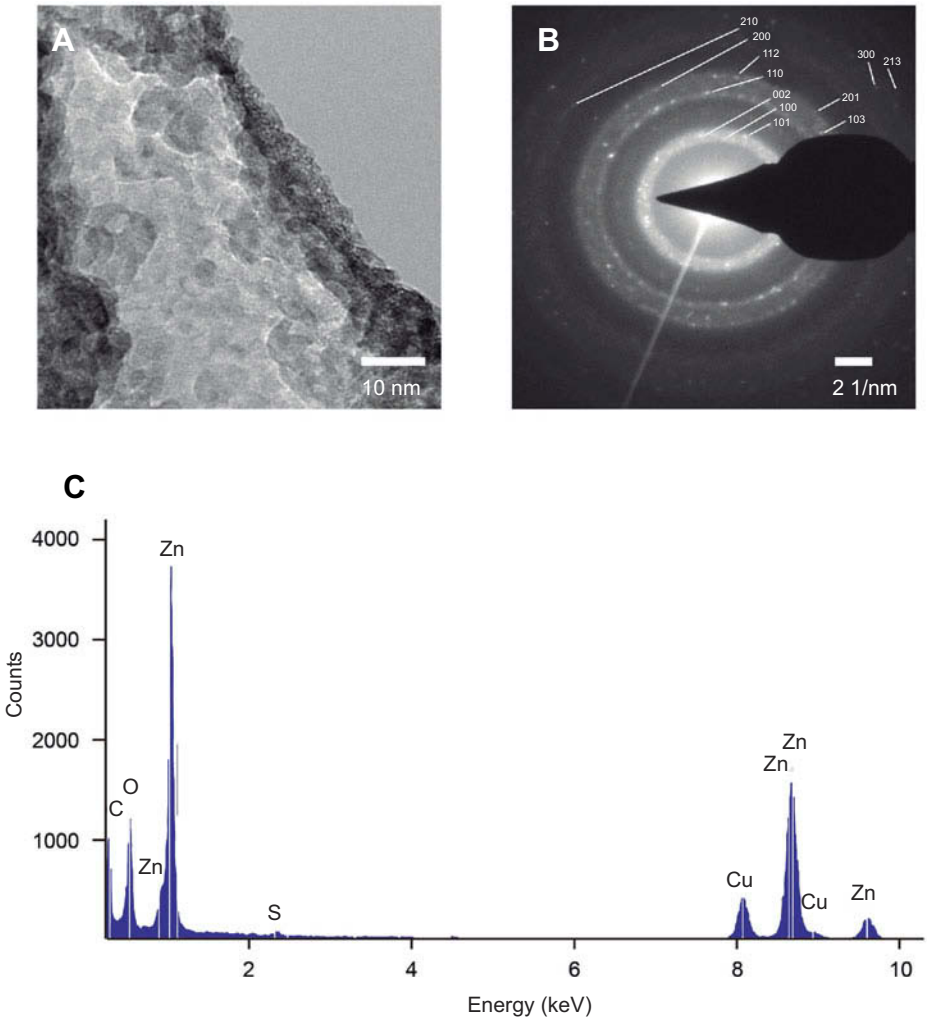

Figure 3 TEM analysis of the synthesized Zn nanoparticles. (**A**) TEM micrography of Zn nanoparticles in the EPS matrix. (**B**) SAED pattern of the synthesized Zn nanoparticles. (**C**) Elemental composition of the ESP capped Zn nanoparticles.
Abbreviations: EPS, exopolysaccharides; TEM, transmission electron microscopy; SAED, selected area electron diffraction.

the metal-EPS biocomposite (Figure 3C). The TEM images of the Ni-EPS biocomposite (Figure 4A) displays, similar to the Zn-EPS biocomposite, a polymorphic arrangement of the capped NPs. These Ni-NPs have a diameter size that ranges from 17 to 52 nm with an average size of 26.73±8.99 nm. A SAED pattern of the EPS-capped NiNPs showed bright rings and spots that correlate to the [1,0,1] plane of a rhombohedral geometry in NiO (Figure 4B). EDS analysis of this Ni-EPS biocomposite demonstrated the presence of Ni, C and O, confirming the presence of these elements in the biocomposite (Figure 4C). Taking a total reduction of Zn(II) ions, the Zn:EPS ratio in a solution of 1 mg/mL is 0.105:0.895 mg. Taking a total reduction of Ni(II) ions, the Ni:EPS ratio in a solution of 1 mg/mL is 0.766:0.234 mg. The zeta potential of the synthesized NPs was −84.3, −8.6 and −76.1 mV for Zn-EPS, Ni-EPS and EPS alone, respectively.

Antimicrobial and antibiofilm activity of EPS-capped metal NPs

We tested antimicrobial and antibiofilm properties at different concentrations of the synthesized biocomposites. In SaR assays treated with the synthesized NiNPs, we found more than 90% of growth inhibition with 3 and 4 mg/mL, up to 80% of growth inhibition was achieved with 2 mg/mL of these NPs and only 20% of inhibition was seen when treated with 1 mg/mL (Figure 5A). Every treatment with NiNPs showed a significant difference ($p<0.05$) when

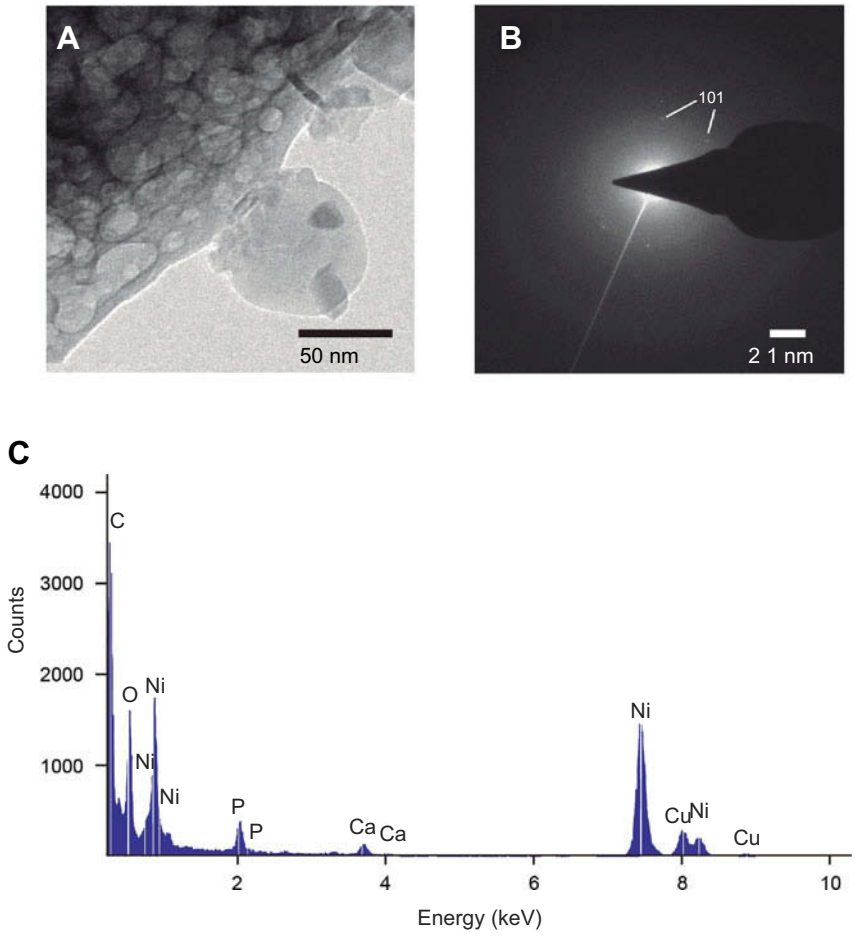

Figure 4 TEM analysis of the synthesized Ni nanoparticles. (**A**) TEM micrography of Ni nanoparticles in the EPS matrix. (**B**) SAED pattern of the synthesized Ni nanoparticles. (**C**) Elemental composition of the ESP capped Ni nanoparticles.
Abbreviations: EPS, exopolysaccharides; TEM, transmission electron microscopy; SAED, selected area electron diffraction.

compared with the untreated control and EPS alone at the same concentration. However, inhibition caused by the treatment with 3 and 4 mg/mL showed no significant difference ($p<0.05$) between them (Figure 5A). When SaR was treated with the synthesized ZnNPs, we found more than 70% of growth inhibition at the concentrations used in this work. The detailed growth inhibition was of 90%, 80%, 70% and 80% with 1, 2, 3 and 4 mg/mL ZnNPs, respectively. Every treatment showed significant difference ($p<0.05$) when compared with the untreated control and the samples treated with EPS alone at the same concentration. Only the assay treated with 3 mg/mL showed significant difference ($p<0.05$) from the concentrations used. When comparing the NiNPs and ZnNPs treatments, only at a concentration of 2 mg/mL there was no significant difference ($p<0.05$) in the growth inhibition, when compared to that of the control.

In PaR assays treated with the synthesized NiNPs, we found more than 90% of growth inhibition when treated with concentrations of 2, 3 and 4 mg/mL and more of 50% of growth inhibition when treated with 1 mg/mL (Figure 5B). Each of the treatments showed significant difference ($p<0.05$) from the untreated control and the EPS alone at the same concentration. There was no significant difference ($p<0.05$) between the growth inhibition caused by the treatment at 2, 3 and 4 mg/mL. On the other hand, the treatments with ZnNPs showed a different behavior than the one exhibited in the assay against *SaR*. We found around 50% of growth inhibition when used at 1 and 2 mg/mL, but no inhibition was found at higher concentrations (Figure 5B). Only the treatment with 3 mg/mL had no significant difference ($p<0.05$) with the untreated control, but every treatment has significant difference ($p<0.05$) with the EPS used at the same concentration. When comparing the inhibition caused by the different NPs, no significant difference ($p<0.05$) was found when used at 1 mg/mL.

Different concentrations of the extracted EPS and the EPS-capped metal NPs were tested as antibiofilm agents. In the *SaR* assays treated with the synthesized NiNPs, the

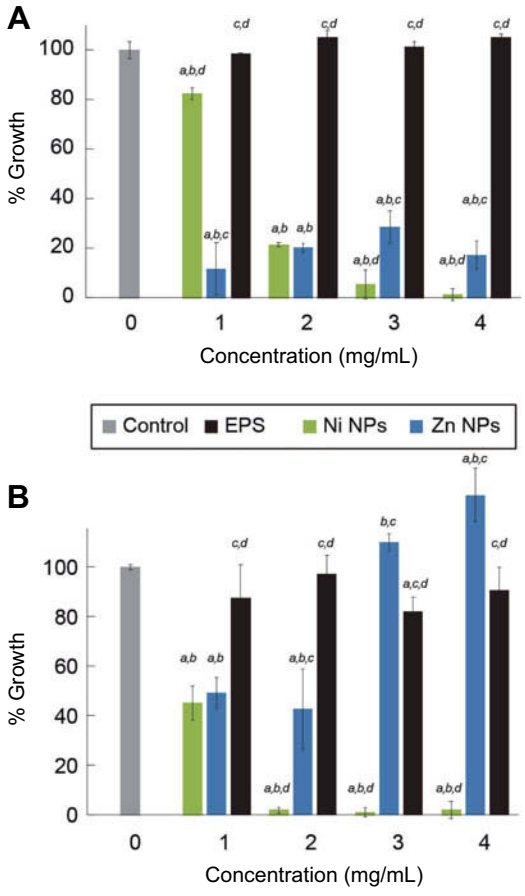

Figure 5 Antimicrobial activity of EPS-capped metal nanoparticles against antibiotic-resistant strains. Growth percentage of bacteria treated with different concentration of metal nanoparticles. (**A**) Effect of the EPS and EPS-capped nanoparticles against SaR. (**B**) Effect of EPS and EPS-capped nanoparticles against PaR. *a* shows significant difference from untreated control. *b* shows significant difference from EPS at the same concentration. *c* shows significant difference from NiNPs at the same concentration. *d* shows significant difference from ZnNPs at the same concentration. Error bars show standard deviation. Every experiment was carried out with replicates of three.
Abbreviation: EPS, exopolysaccharides.

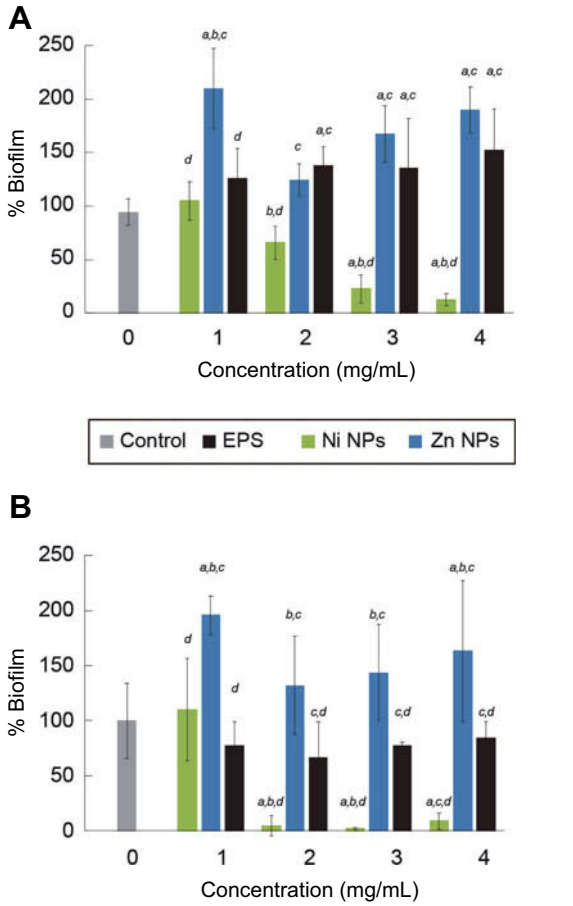

Figure 6 Antibiofilm activity of EPS-capped metal nanoparticles against antibiotic-resistant strains. Biofilm formation percentage of bacteria treated with different concentration of metal nanoparticles. (**A**) Effect of the EPS and EPS-capped nanoparticles against SaR. (**B**) Effect of EPS and EPS-capped nanoparticles against PaR. *a* shows significant difference from untreated control. *b* shows significant difference from EPS at the same concentration. *c* shows significant difference from NiNPs at the same concentration. *d* shows significant difference from ZnNPs at the same concentration. Error bars show standard deviation. Every experiment was carried out with replicates of three.
Abbreviation: EPS, exopolysaccharides.

biofilm formation was inhibited up to 80% and 90% when a concentration of 3 and 4 mg/mL was used, respectively (Figure 6A). These two treatments showed significant difference ($p<0.05$) with the untreated control and the EPS alone. When treated with either the extracted EPS or the synthesized ZnNPs, no biofilm inhibition ($p<0.05$) was found and increased production was observed. When comparing the biofilm inhibition caused by the different NPs, a significant difference ($p<0.05$) was found at every concentration used.

In the PaR antibiofilm assays, performed with the synthesized NiNPs, we found more than 90% of inhibition when treated with 2, 3 and 4 mg/mL with no significant difference ($p<0.05$) between them. Only the bacteria treated with 1 mg/mL showed no significant difference ($p<0.05$) with the untreated control. On the other hand, an increased biofilm production was observed when the bacteria was treated with the synthesized ZnNPs; similar results were observed for the assays against SaR. No significant ($p<0.05$) biofilm inhibition was found when treated with EPS alone. The treatments with NiNPs at 2, 3 and 4 mg/mL showed significant difference ($p<0.05$) with the extracted EPS at the same concentrations.

Antibacterial mechanism of EPS-capped NPs

To understand the antimicrobial effects of the EPS-capped NPs, we treated the strains with each synthesized composite in order to measure leakage of intracellular compounds; such is the case of reducing sugars. Considering the untreated control as 0% of leaked sugars, when treating SaR with each composite we observed a general increased percentage

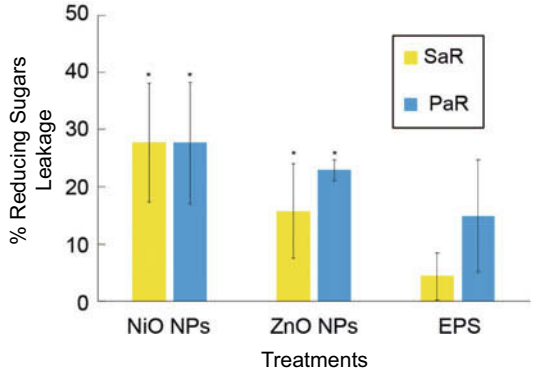

Figure 7 The effect of EPS-capped NiO, ZnO composites on the membrane leakage of reducing sugars to the culture media. Percentage increment of leaked reducing sugars to the culture media of SaR and PaR caused by the exposure of both synthesized composites and EPS at 3 mg/mL, and comparing to an untreated control. Error bars show standard deviation. * indicates significant difference ($p<0.05$) compared to the untreated control. Every experiment was carried out with replicates of three.
Abbreviation: EPS, exopolysaccharides.

of reducing sugars in the media for all of the EPS NP treatments. The increased percentages observed were 27.69%, 15.74% and 4.34% when using NiONPs, ZnONPs and EPS, respectively (Figure 7). When treating PaR with each composite, we observed similar results; the generalized increment in the media was 27.63%, 22.85% and 14.88% using NiONPs, ZnONPs and EPS treatments, respectively (Figure 7). For both strains and in both treatments with the EPS-capped NPs, the results show significant differences ($p<0.05$) when compared with the untreated control; moreover, the EPS treatments in both strains showed no significant difference when compared to the control.

In vivo toxicological study

Oral treatment with EPS, Ni and Zn NPs was performed to test the toxicity of the synthesized EPS-capped metal NPs. For the toxicity study, different parameters of renal function were evaluated, including urinary volume, urinary concentrations of proteins, glucose and creatinine, as well as blood concentrations of creatinine. Figure 8 shows that in the urinary volume (Figure 8A), glucose (Figure 8B) and proteins (Figure 8C) there is no significant difference ($p<0.05$) between the control, EPS and NPs-treated groups. Similarly, the EPS and NPs groups showed statistical similarity ($p<0.05$) in the creatinine concentrations in both urine and plasma (Figure 8D and E, respectively) with the untreated control group.

Finally, no differences were observed in the appearance and behavior between the treated and untreated animals.

Discussion

Exopolysaccharide extracted from Rhodotorula mucilaginosa UANL-001L

FTIR analysis of the EPS (Figure 1) shows a broad band between 3600 and 3200 cm^{-1}, wavenumber that has been ascribed to O–H functional groups in alcohols. A band at 2900 cm^{-1} is also shown and it is related to the stretch of CH_3. The band that appears at 1650 cm^{-1} is attributed to a C=O stretch.[43] The bands around 1420 cm^{-1} are linked to the C–H bending in backbones of carbohydrates. The weak band at 1350 cm^{-1} is related to carboxyl groups. The bands around 1250–1050 cm^{-1} have been related to stretching vibration of C–O–C in sugar derivates.[44] Altogether, these results suggest that the synthesized EPS contains mainly saccharides and carboxylates, as we have previously reported.[42]

EPS-capped Zn and Ni NPs synthesis and characterization

A color change was observed after the redox reaction between the different transition metal salts and ascorbic acid, in the presence of EPS. The products from the reactions were analyzed using UV-Vis spectroscopy. The UV-Vis spectra displayed SPR characteristic absorption peaks (Figure 2) with maximums at 347 and 348 nm for the reactions containing Zn and Ni, respectively. These results demonstrate evidence that there is NPs synthesis since SPR UV-Vis absorption peaks for ZnNPs (ZnO) and NiNPs (NiO) have been observed at a range between 334–375 nm[45–47] and 320–360 nm,[48–50] respectively. Furthermore, the UV-Vis spectra of a Zn(II) solution and that of a Ni(II) solution, at the same concentrations used for the NP synthesis, showed no absorption peak at those wavelengths. Moreover, Ni^{2+} has a strong absorption peak around 400 nm and two more around 650–750 nm;[51] after the redox reaction, there is a reduction in the absorbance at 400 nm (Figure 2), suggesting the formation of NiNPs as Ni ions concentration decrease (Figure 2).

To further confirm that the EPS functions as a capping agent in the NP synthesis, the samples were analyzed with a FT-IR. As can be observed from Figure 1, there are no new peaks observed in the samples after the redox reaction in the presence of EPS; however, wavenumber shifts and attenuation of the intensities of some absorption peak were observed. For both Ni and Zn redox reactions, the C=O peak absorbs at lower wavelength number due to NPs conjugation. Furthermore, C–H bands become weaker

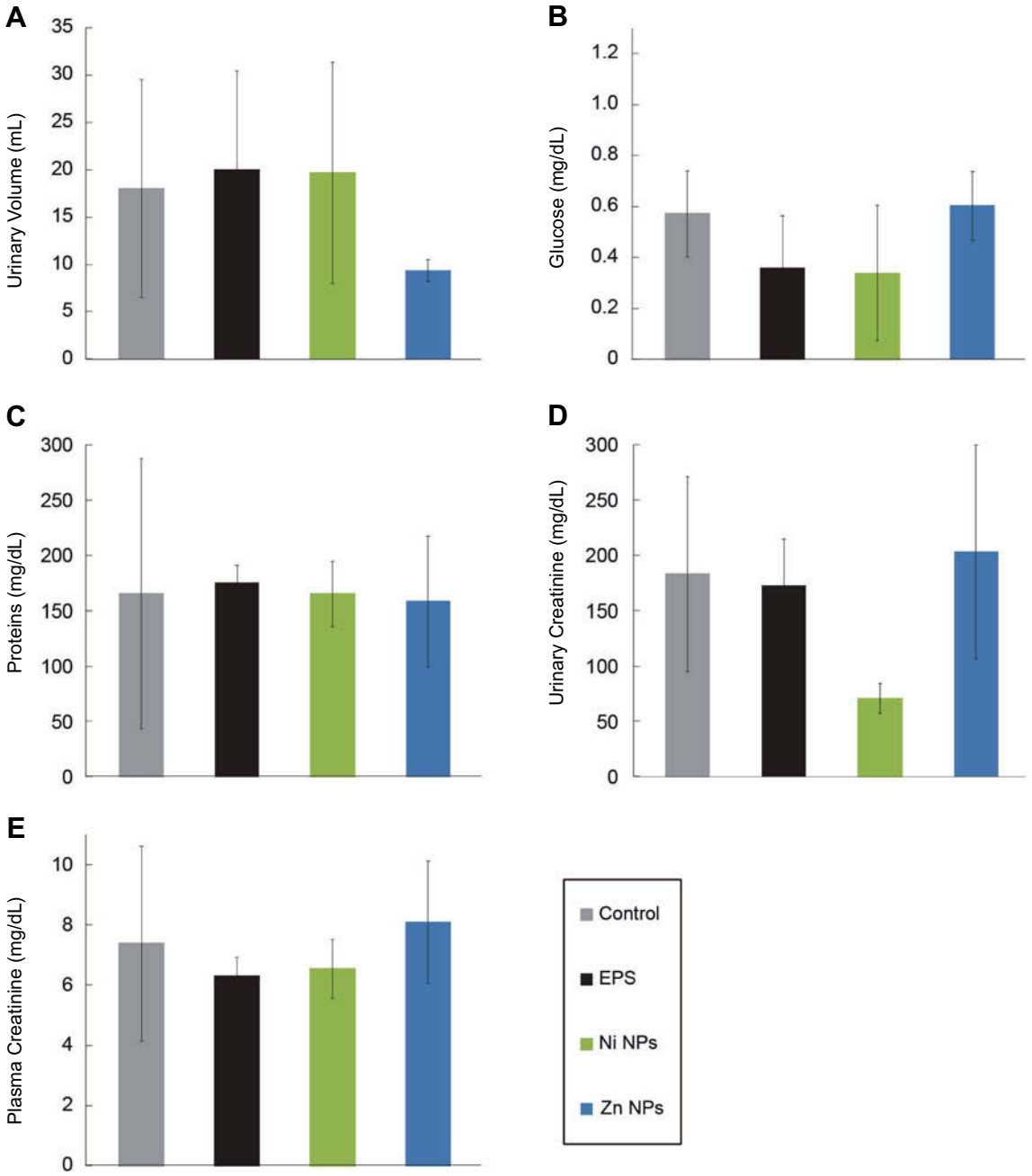

Figure 8 Parameters of renal function of Wistar rats treated with EPS-capped Ni and Zn nanoparticles. Test was performed treating rats with 6 mg/mL of buffer (control), EPS, NiNPs and ZnNPs. (**A**) urinary volume, (**B**) glucose, (**C**) total proteins, (**D**) urinary creatinine and (**E**) plasma creatinine. Error bars show standard deviation. Every experiment was carried out with replicates of three.

Abbreviation: EPS, exopolysaccharides.

which suggests that the NPs have an interaction with the hydrogen bonds in the polysaccharides.[27] Similarly, C–O–C bands become weaker but C–O peaks around 1300 cm^{-1} become stronger when compared to the pure EPS before the reactions; these results indicate that some sugars of the EPS are involved in the reduction of the metal ions,[52] which in the redox reaction work together with the effect of the ascorbic acid.

The synthesized metal NP composites were also characterized by TEM (Figure 3A) and SAED. For the ZnNPs, we calculated an average particle size diameter of 8.32 nm. Furthermore, the SAED displays bright diffusive dotted rings which identify the [1,0,0], [0,0,2], [1,0,1], [1,1,0], [1,0,3], [2,0,0], [1,1,2], [2,0,1], [2,1,0], [3,0,0] and [2,1,3] planes (Figure 3B). These planes correspond to a hexagonal geometry in ZnO NPs (JCPDS No. 36–1451).[45,52,53]

Furthermore, EDS confirmed the presence of Zn and organic compounds in our metal NP composites (Figure 3C). The organic compounds found in the EPS and the Zn from the NPs. Similar characterization was performed of the Ni NP composites with TEM and SAED; we calculated an average particle size diameter of 26.73 nm, and the SAED results showed (Figure 4B) two strongly diffusive rings, and just one dot ring; this allowed the [1,0,1] plane to be identified. This plane corresponds to a rhombohedral geometry NiO NPs (JCPDS No. 44–1159).[54,55] By EDS (Figure 4C) we observed the presence of Ni as well as other organic compounds that correlate to those found in EPS. In both EDS samples, Cu appears due to the fact that the samples are analyzed on top of a copper grid. For both samples, bright diffusive rings in SAED patterns were found; as part of the amorphous EPS structure, these rings can be found in amorphous materials, and the diffraction rings found in our samples are characteristic of polycrystalline materials.[56]

Antimicrobial and antibiofilm activity of EPS-capped metal NPs

NPs have a wide array of biomedical applications. Many different metal NPs such as TiO_2, Ag, ZnO, CuO, MgO, etc. have been reported as potential antimicrobial agents.[57] Moreover, EPS have different effects in bacterial growth, which depends on the functional groups it presents in their backbone. These effects of EPS on bacterial growth can be antagonistic[58] productive or neutral[59] and their effects also depend on the bacterial strain. Here we tested the antimicrobial activity of the synthesized NPs capped in the EPS matrix against two relevant clinical pathogenic strains, a resistant Gram-positive *Staphylococcus aureus* and a resistant Gram-negative *Pseudomonas aeruginosa*. We previously showed that the EPS has no inhibitory effect against the clinical strains used in the current work, but the EPS-capped NiNPs metal nanocomposites were capable of inhibiting, in a dose-response manner, both bacterial strains; PaR *and* SaR at 2 and 3 mg/mL, respectively. Inhibitory effect of Ni ions, Ni- and NiO have been compared against oral infecting bacteria and the results show that Ni NPs had the lowest effective antimicrobial activity among the mentioned agents.[60] However, here we demonstrate that the metal NP composite containing NiO NPs showed better antimicrobial activity than EPS alone, against both Gram-positive and Gram-negative bacteria (Figure 5), inhibiting up to 99% at 3 and 2 mg/mL, respectively. These effects, where the composite exhibits a higher inhibition when compared to the polymer alone, have been observed for other metal-polymer compounds;[61] this effect has been suggested to be a surfactant effect from the EPSs.[62] A very similar effect was observed in regard to the antimicrobial activity of EPS-capped Zn NPs (Figure 5), where we demonstrated different inhibitory capacity according to each strain. This EPS nanocomposite was capable of inhibiting up to 90% of the SaR population at 1 mg/mL but only 50% of inhibition when used against PaR at the same concentration. Metal NPs have different activity against bacteria depending on the size and capping agent, due to their well-known difference cell wall composition.[63–68] Accordingly, we observed that the NPs synthesized in this work showed different activity against Gram-positive and Gram-negative bacteria. ZnO-EPS composite showed more activity against Gram-positive bacteria than NiO-EPS composite, and NiO-EPS composite showed more activity against Gram-negative bacteria than ZnO-EPS composite.

As mentioned above, an interesting feature of some microbial EPS is their potential use as antibiofilm agents.[69] However, the EPS of *R. mucilaginosa* UANL-001L showed no antibiofilm activity against the clinical *P. aeruginosa* strain and an increase in biofilm formation was observed when the clinical *S. aureus* strain was treated with EPS (Figure 6). This may be related to the multifactorial mechanisms involved in biofilm formation.[70] When tested against SaR, ZnNPs did not have any antibiofilm activity, contrary to what was expected due to its potent antimicrobial activity. These results agree with some of the literature where ZnO NPs alone displays antimicrobial effects but do not show antibiofilm activity against a variety of strains.[71] However, the NiNPs polymer composites displayed very interesting antibiofilm results (Figure 6). For the case of SaR, samples treated with NiNPs showed a gradual decrease in biofilm production as the composite concentration is increased, inhibiting up to 90% at 3 mg/mL; however, when tested against PaR there is a rapid decrease in biofilm formation from 110% to 4.5% when using 1 and 2 mg/mL of the NiNPs biocomposites, respectively. Both cases showed the same behavior to the antimicrobial tests; thus, the gradual decrease of SaR growth and the rapid inhibition of PaR growth were reported. Against both clinical strains, little production of biofilm was maintained, even when the metal NPs exhibited almost a complete growth inhibition at the same concentration. This kind of behavior was also

observed by Saleem et al.[72] with NiO NPs. They tested the antimicrobial and antibiofilm activity of green-synthesized NiO NPs against a variety of clinical strains and observed biofilm production even at reported inhibitory concentrations.

Antibacterial mechanism of EPS-capped NPs

The release of intracellular water-soluble compounds to the culture media has been used to determine the integrity of cell wall when bacteria is exposed to antimicrobial agents. Release of intracellular compounds has been proposed as a possible antimicrobial mechanism of microbial polysaccharides[73] and modified polysaccharides.[74] In the present study, we observed an increased percentage of soluble reducing sugars in culture media after incubation with the synthesized composites using an inhibitory concentration, suggesting that the bacteria membrane could be one of the antimicrobial targets of the synthesized composites. A positive charged particle has more electrostatic interaction with negatively charged cellular membranes,[75] but also negative charged particles have been reported to absorb negative compounds as proteins.[76] As the zeta potential measurements indicate, the synthesized composites have negative charge, but when the NiONPs were synthesized the potential changed from −76.1 to −8.6 mV, suggesting that NiONPs could have positive charge. This could be the reason for the higher antimicrobial activity and leakage of reducing sugars to the media caused by NiO-EPS composite.

In vivo toxicological study

When testing antimicrobial and antibiotic effects of different compounds, it is necessary to assess that the therapeutic compounds do not disrupt appropriate functioning of biological activities. In many cases, an assessment on kidney and liver function, after being challenged with the therapeutic, represents a proper first step towards determining the potential and relevance of the compound for biomedical applications. The nephrons are the basic structural and functional units, as they carry out the glomerular filtration, the tubular reabsorption and the tubular secretion.[77] Here, we assessed several renal function parameters in urine, such as volume (amount of body fluid), concentration of glucose (associated with tubular function), concentration of total proteins (associated with glomerular filtration and general function of nephrons) and the concentration of creatinine in both plasma and urine (linked with glomerular filtration rate) in the organism.

Several studies have shown toxicity of metal NPs, such as Zn,[78] but other studies have shown that metal NPs such as NiNPs are innocuous.[79] In many cases, the synthesis method is crucial in the toxicity outcome of the NPs and the main purpose of using green synthesis methods is to increase their biocompatibility. In this work, we have purposely used green synthesis methods to decrease the possible toxicity of the synthesized metal polymer nanocomposites. As can be observed in the results in Figure 8, after a group of rats were treated orally in a three-day regimen with 6 mg/mL (24 mg/kg of body weight) of both EPS NiNPs and ZnNPs composites; all of the parameters showed no significant difference when compared to the control group. This dose is below the LD50 reported for these metal oxide NPs, even below of some NOAEL concentrations of a *Rhodotorula minuta* EPS.[80–83] Thus, the results suggest that the EPS-capped NiO, and ZnO NPs synthesized in this study do not produce any toxic or adverse effect in the nephrons and renal function of the treated animals.

Conclusion

The exopolysaccharide extracted from *Rhodotorula mucilaginosa* UANL-001L culture can be used as a capping agent in the synthesis of Zn and Ni NPs. The synthesized metal NPs were obtained as oxides, *eg* ZnO and NiO NPs. EPS-capped NiO NPs were capable to inhibit more than 90% growth of two clinical strains, a resistant Gram-negative *Pseudomonas aeruginosa* and a resistant Gram-positive *Staphylococcus aureus* at 2 and 3 mg/mL, respectively. These metal NPs were also capable to inhibit the biofilm formation up to 90% of both clinical strains at the inhibitory concentrations. EPS-capped ZnO NPs were capable to inhibit 90% growth of the resistant *Staphylococcus aureus* clinical strain but only up to 50% of the resistant *Pseudomonas aeruginosa* clinical strain. However, the Zn NPs EPS biocomposites had no capacity to inhibit the biofilm formation of any of the clinical strains used in this study. Both composites were capable of increasing the amount of soluble reducing sugars in the culture media, suggesting the bacterial membrane as an antimicrobial target. Furthermore, both of the EPS-capped metal NPs showed no toxic effect *in* vivo. Taken together, our results suggest that EPS-capped NiO NPs can be useful as antimicrobial and antibiofilm agents against clinical strains.

Acknowledgments

The Universidad Autónoma de Nuevo León and CONACyT for providing financial support through Paicyt 2016-2017 Science Grant from the Universidad Autónoma de Nuevo León. CONACyT Grants for: Basic science grant 221332, Fronteras de la Ciencia grant 1502 and Infraestructura Grant 279957.

Author contributions

JAGC, CEEG, GMG and JRMR designed, performed and analyzed the experimental data and wrote the article. EDBC designed and performed the TEM analysis and contributed to the discussion and format of the article. BAMC and MALV designed and performed partially the *in vivo* toxicity experiments. All authors contributed to data analysis, drafting or revising the article, gave final approval of the version to be published, and agree to be accountable for all aspects of the work.

Disclosure

The authors reports no conflicts of interest in this work.

References

1. Wohlleben W, Mast Y, Stegmann E, Ziemert N. Antibiotic drug discovery. *Microb Biotechnol*. 2016;9(5):541–548. doi:10.1111/1751-7915.12388
2. Pendleton JN, Gorman SP, Gilmore BF. Clinical relevance of the ESKAPE pathogens. *Expert Rev Anti Infect Ther*. 2013;11 (3):297–308. doi:10.1586/eri.13.12
3. Bell BG, Schellevis F, Stobberingh E, Goossens H, Pringle M. A systematic review and meta-analysis of the effects of antibiotic consumption on antibiotic resistance. *BMC Infect Dis*. 2014;14(1):13. doi:10.1186/1471-2334-14-13
4. Spellberg B, Powers JH, Brass EP, Miller LG, Edwards JE. Trends in antimicrobial drug development: implications for the future. *Clin Infect Dis*. 2004;38(9):1279–1286. doi:10.1086/420937
5. Kumar A, Alam A, Rani M, Ehtesham NZ, Hasnain SE. Biofilms: survival and defense strategy for pathogens. *Int J Med Microbiol*. 2017;307(8):481–489. doi:10.1016/j.ijmm.2017.09.016
6. Otter JA, Vickery K, Walker JT, et al. Surface-attached cells, biofilms and biocide susceptibility: implications for hospital cleaning and disinfection. *J Hosp Infect*. 2015;89(1):16–27. doi:10.1016/j.jhin.2014.09.008
7. Vickery K, Deva A, Jacombs A, Allan J, Valente P, Gosbell IB. Presence of biofilm containing viable multiresistant organisms despite terminal cleaning on clinical surfaces in an intensive care unit. *J Hosp Infect*. 2012;80(1):52–55. doi:10.1016/j.jhin.2011.07.007
8. Rybtke M, Hultqvist LD, Givskov M, Tolker-Nielsen T. Pseudomonas aeruginosa biofilm infections: community structure, antimicrobial tolerance and immune response. *J Mol Biol*. 2015;427(23):3628–3645. doi:10.1016/j.jmb.2015.08.016
9. Holban AM, Gestal MC, Grumezescu AM. Control of biofilm-associated infections by signaling molecules and nanoparticles. *Int J Pharm*. 2016;510(2):409–418. doi:10.1016/j.ijpharm.2016.02.044
10. Béguin P. An introduction to polysaccharide biotechnology. *Biochimie*. 1998;80(4):347. doi:10.1016/S0300-9084(98)80079-5
11. Rendueles O, Kaplan JB, Ghigo J-M. Antibiofilm polysaccharides. *Environ Microbiol*. 2013;15(2):334–346. doi:10.1111/j.1462-2920.2012.02810.x
12. Bernal P, Llamas MA. Promising biotechnological applications of antibiofilm exopolysaccharides. *Microb Biotechnol*. 2012;5 (6):670–673. doi:10.1111/j.1751-7915.2012.00359.x
13. Valle J, Da Re S, Henry N, et al. Broad-spectrum biofilm inhibition by a secreted bacterial polysaccharide. *PNAS*. 2006;103 (33):12558–12563. doi:10.1073/pnas.0605399103
14. Golberg K, Emuna N, Vinod TP. et al. Novel anti-adhesive biomaterial patches: preventing biofilm with Metal Complex Films (MCF) derived from a microalgal polysaccharide. *Adv Mater Interfaces*;2016. 1500486. doi:10.1002/admi.201500486
15. Pal S, Yoon EJ, Park SH, Choi EC, Song JM. Metallopharmaceuticals based on silver (I) and silver (II) polydiguanide complexes: activity against burn wound pathogens. *J Antimicrob Chemother*. 2010;65 (10):2134–2140. doi:10.1093/jac/dkq294
16. Morones JR, Elechiguerra JL, Camacho A, et al. The bactericidal effect of silver nanoparticles. *Nanotechnology*. 2005;16(10):2346. doi:10.1088/0957-4484/16/10/059
17. Xu FF, Imlay JA. Silver (I), mercury (II), cadmium (II), and zinc (II) target exposed enzymic iron-sulfur clusters when they toxify Escherichia coli. *Appl Environ Microbiol*. 2012;78(10):3614–3621. doi:10.1128/AEM.07368-11
18. Stanić V, Dimitrijević S, Antić-Stanković J, et al. Synthesis, characterization and antimicrobial activity of copper and zinc-doped hydroxyapatite nanopowders. *Appl Surf Sci*. 2010;256(20):6083–6089. doi:10.1016/j.apsusc.2010.03.124
19. Bajpai SK, Chand N, Chaurasia V. Nano zinc oxide-loaded calcium alginate films with potential antibacterial properties. *Food Bioprocess Technol*. 2012;5(5):1871–1881. doi:10.1007/s11947-011-0587-6
20. Das P, Ganguly S, Bose M, et al. Zinc and nitrogen ornamented bluish white luminescent carbon dots for engrossing bacteriostatic activity and Fenton based bio-sensor. *Mater Sci Eng C*. 2018;88:115–129. doi:10.1016/J.MSEC.2018.03.010
21. Maeda T, Negishi A, Nogami Y, Sugio T. Nickel inhibition of the growth of a sulfur-oxidizing bacterium isolated from corroded concrete. *Biosci Biotechnol Biochem*. 1996;60(4):626–629. doi:10.1271/bbb.60.626
22. Argueta-Figueroa L, Morales-Luckie RA, Scougall-Vilchis RJ, Olea-Mej??a OF. Synthesis, characterization and antibacterial activity of copper, nickel and bimetallic Cu-Ni nanoparticles for potential use in dental materials. *Prog Nat Sci Mater Int*. 2014;24(4):321–328. doi:10.1016/j.pnsc.2014.07.002
23. Garza-Cervantes JA, Chávez-Reyes A, Castillo EC, et al. Synergistic antimicrobial effects of silver/transition-metal combinatorial treatments. *Sci Rep*. 2017;7(1). doi:10.1038/s41598-017-01017-7
24. Morones-Ramirez JR, Winkler JA, Spina CS, Collins JJ. Silver enhances antibiotic activity against gram-negative bacteria. *Sci Transl Med*. 2013;5(190):190ra81. doi:10.1126/scitranslmed.3006276
25. Park Y, Hong YN, Weyers A, Kim YS, Linhardt RJ. Polysaccharides and phytochemicals: a natural reservoir for the green synthesis of gold and silver nanoparticles. *IET Nanobiotechnol*. 2011;5(3):69. doi:10.1049/iet-nbt.2010.0033
26. Duan H, Wang D, Li Y. Green chemistry for nanoparticle synthesis. *Chem Soc Rev*. 2015. doi:10.1039/c4cs00363b
27. Sathiyanarayanan G, Dineshkumar K, Yang Y-H. Microbial exopolysaccharide-mediated synthesis and stabilization of metal nanoparticles. *Crit Rev Microbiol*. 2017;1–22. doi:10.1080/1040841X.2017.1306689
28. Panigrahi S, Kundu S, Ghosh SK, Nath S, Pal T. General method of synthesis for metal nanoparticles. *J Nanoparticle Res*. 2004. doi:10.1007/s11051-004-6575-2

29. Saha S, Pal A, Kundu S, Basu S, Pal T. Photochemical green synthesis of calcium-alginate-stabilized ag and au nanoparticles and their catalytic application to 4-nitrophenol reduction. *Langmuir*. 2010. doi:10.1021/la902950x
30. Ganguly S, Mondal S, Das P, et al. Natural saponin stabilized nano-catalyst as efficient dye-degradation catalyst. *NanoStruct NanoObjects*. 2018;16:86–95. doi:10.1016/J.NANOSO.2018.05.002
31. Das TK, Bhawal P, Ganguly S, Mondal S, Das NC. A facile green synthesis of amino acid boosted Ag decorated reduced graphene oxide nanocomposites and its catalytic activity towards 4-nitrophenol reduction. *Surf Interfaces*. 2018;13:79–91. doi:10.1016/J.SURFIN.2018.08.004
32. Cao G, Wang Y. *Nanostructures and Nanomaterials*. World Scientific; 2011; doi:10.1142/7885
33. Makarov VV, Love AJ, Sinitsyna OV, et al. "Green" nanotechnologies: synthesis of metal nanoparticles using plants. *Acta Naturae*. 2014;6(20):35–44. doi:10.1039/c1gc15386b
34. Kanmani P, Lim ST. Synthesis and structural characterization of silver nanoparticles using bacterial exopolysaccharide and its antimicrobial activity against food and multidrug resistant pathogens. *Process Biochem*. 2013;48(7):1099–1106. doi:10.1016/j.procbio.2013.05.011
35. Chen X, Yan J-K, Wu J-Y. Characterization and antibacterial activity of silver nanoparticles prepared with a fungal exopolysaccharide in water. *Food Hydrocoll*. 2015;53:69–74. doi:10.1016/j.foodhyd.2014.12.032
36. Miller GL. Use of dinitrosalicylic acid reagent for determination of reducing sugar. *Anal Chem*. 1959. doi:10.1021/ac60147a030
37. O'Toole GA. Microtiter dish biofilm formation assay. *J Vis Exp*. 2011;(47). doi:10.3791/2437
38. Trinder P. Determination of glucose in blood using glucose oxidase with an alternative oxygen acceptor. *Ann Clin Biochem*. 1966;6(1), 24–27.
39. Gornall AG, Bardawill CJ, David MM. Determination of serum proteins by means of the biuret reaction. *J Biol Chem*. 1949;177 (2):751–766. doi:10.5555/URI:PII:0022214349903054
40. Rartels H, Böhmer M. Eine mikromethode 7air kreatininbestimmung. *Clin Chim Acta*. 1971;32(1):81–85. doi:10.1016/0009-8981(71)90467-0
41. Fabiny DL, Ertingshausen G. Automated reaction-rate method for determination of serum creatinine with the CentrifiChem. *Clin Chem*. 1971;17(8):696–700.
42. Vazquez-Rodriguez A, Vasto-Anzaldo XG, Barboza Perez D, et al. Microbial competition of rhodotorula mucilaginosa uanl-0011 and E. coli increase biosynthesis of non-toxic exopolysaccharide with applications as a wide-spectrum antimicrobial. *Sci Rep*. 2018;8 (1):798. doi:10.1038/s41598-017-17908-8
43. Garza MTG, Perez DB, Rodriguez AV, et al. Metal-induced production of a novel bioadsorbent exopolysaccharide in a native rhodotorula mucilaginosa from the mexican northeastern region. *PLoS One*. 2016;11(2):e0148430. doi:10.1371/journal.pone.0148430
44. Wang Q, Kang F, Gao Y, Mao X, Hu X. Sequestration of nanoparticles by an EPS matrix reduces the particle-specific bactericidal activity. *Sci Rep*. 2016;6. doi:10.1038/srep21379
45. Talam S, Karumuri SR, Gunnam N. Synthesis, characterization, and spectroscopic properties of ZnO nanoparticles. *ISRN Nanotechnol*. 2012;2012:1–6. doi:10.5402/2012/372505
46. Kumar SS, Venkateswarlu P, Rao VR, Rao GN. Synthesis, characterization and optical properties of zinc oxide nanoparticles. *Int Nano Lett*. 2013;3(1):30. doi:10.1186/2228-5326-3-30
47. Sangeetha G, Rajeshwari S, Venckatesh R. Green synthesis of zinc oxide nanoparticles by aloe barbadensis miller leaf extract: structure and optical properties. *Mater Res Bull*. 2011;46(12):2560–2566. doi:10.1016/j.materresbull.2011.07.046
48. Salavati-Niasari M, Davar F, Fereshteh Z. Synthesis of nickel and nickel oxide nanoparticles via heat-treatment of simple octanoate precursor. *J Alloys Compd*. 2010;494(1–2):410–414. doi:10.1016/j.jallcom.2010.01.063
49. Salavati-Niasari M, Mir N, Davar F. A novel precursor in preparation and characterization of nickel oxide nanoparticles via thermal decomposition approach. *J Alloys Compd*. 2010;493(1–2):163–168. doi:10.1016/j.jallcom.2009.11.153
50. Dharmaraj N, Prabu P, Nagarajan S, Kim CH, Park JH, Kim HY. Synthesis of nickel oxide nanoparticles using nickel acetate and poly (vinyl acetate) precursor. *Mater Sci Eng B Solid-State Mater Adv Technol*. 2006;128(1–3):111–114. doi:10.1016/j.mseb.2005.11.021
51. Ibrahim MAM, Al Radadi RM. Role of glycine as a complexing agent in nickel electrodeposition from acidic sulphate bath. *Int J Electrochem Sci*. 2015;10:4946–4971. www.electrochemsci.org. Accessed, 2018.
52. Kang F, Alvarez PJ, Zhu D. Microbial extracellular polymeric substances reduce Ag^{+} to silver nanoparticles and antagonize bactericidal activity. *Environ Sci Technol*. 2014;48(1):316–322. doi:10.1021/es403796x
53. Aneesh PM, Vanaja KA, Jayaraj MK. Synthesis of ZnO nanoparticles by hydrothermal method. *Proc SPIE*. 2007;6639(6639):66390. doi:10.1117/12.730364
54. Kalyani P, Kalaiselvi N. Various aspects of LiNiO2 chemistry: a review. *Sci Technol Adv Mater*. 2005;6(6):689–703. doi:10.1016/j.stam.2005.06.001
55. Hotovy I, Huran J, Spiess L. Characterization of sputtered NiO films using XRD and AFM. *J Mater Sci*. 2004;39(7):2609–2612. doi:10.1023/B:JMSC.0000020040.77683.20
56. Suvorova EI, Buffat PA. Electron diffraction from micro- and nanoparticles of hydroxyapatite. *J Microsc*. 1999;196(1):46–58. doi:10.1046/j.1365-2818.1999.00608.x
57. Parham S, Wicaksono DHB, Bagherbaigi S, Lee SL, Nur H. Antimicrobial treatment of different metal oxide nanoparticles: a critical review. *J Chinese Chem Soc*. 2016;63(4):385–393. doi:10.1002/jccs.201500446
58. Onbasli D, Aslim B. Determination of antimicrobial activity and production of some metabolites by Pseudomonas aeruginosa B1 and B2 in sugar beet molasses. *African J Biotechnol*. 2008;7 (24):4614–4619. doi:10.5897/AJB08.691
59. Liang TW, Wu CC, Cheng WT, et al. Exopolysaccharides and antimicrobial biosurfactants produced by paenibacillus macerans TKU029. *Appl Biochem Biotechnol*. 2014;172(2):933–950. doi:10.1007/s12010-013-0568-5
60. Khan ST, Ahamed M, Alhadlaq HA, Musarrat J, Al-Khedhairy A. Comparative effectiveness of NiCl2, Ni- and NiO-NPs in controlling oral bacterial growth and biofilm formation on oral surfaces. *Arch Oral Biol*. 2013;58(12):1804–1811. doi:10.1016/j.archoralbio.2013.09.011
61. Sambhy V, MacBride MM, Peterson BR, Sen A. Silver bromide nanoparticle/polymer composites: dual action tunable antimicrobial materials. *Journal of the American Chemical Society*. 2006;128 (30):9798–9808. doi:10.1021/JA061442Z
62. Yilmaz ES, Sidal U. Investigation of antimicrobial effects of a Pseudomonas-originated biosurfactant. *Biol Bratislava*. 2005;60 (6):723–725.
63. Premanathan M, Karthikeyan K, Jeyasubramanian K, Manivannan G. Selective toxicity of ZnO nanoparticles toward Gram-positive bacteria and cancer cells by apoptosis through lipid peroxidation. *Nanomed Nanotechnol*. 2011. doi:10.1016/j.nano.2010.10.001
64. Brayner R, Ferrari-Iliou R, Brivois N, Djediat S, Benedetti MF, Fiévet F. Toxicological impact studies based on Escherichia coli bacteria in ultrafine ZnO nanoparticles colloidal medium. *Nano Lett*. 2006. doi:10.1021/nl052326h
65. Jin T, Sun D, Su JY, Zhang H, Sue HJ. Antimicrobial efficacy of zinc oxide quantum dots against Listeria monocytogenes, Salmonella Enteritidis, and Escherichia coli O157:H7. *J Food Sci*. 2009. doi:10.1111/j.1750-3841.2008.01013.x
66. Emami-Karvani Z, Chehrazi P. Antibacterial activity of ZnO nanoparticle on Gram-positive and Gram-negative bacteria. *African J Microbiol Res*. 2011. doi:10.5897/AJMR10.159

67. Hosseinkhani P, Zand AM, Imani S, Rezayi M, Rezaei Zarchi S. Determining the antibacterial effect of ZnO nanoparticle against the pathogenic bacterium, Shigella dysenteriae (type 1). *Int J Nano Dimens*. 2011;1(4):279–285. doi:10.7508/IJND.2010.04.006
68. Das P, Bose M, Ganguly S, et al. Green approach to photoluminescent carbon dots for imaging of gram-negative bacteria Escherichia coli. *Nanotechnology*. 2017. doi:10.1088/1361-6528/aa6714
69. Qin Z, Yang L, Qu D, Molin S, Tolker-Nielsen T. Pseudomonas aeruginosa extracellular products inhibit staphylococcal growth, and disrut established biofilms produced by staphylococcus epidermidis. *Microbiology*. 2009;155(7):2148–2156. doi:10.1099/mic.0.028001-0
70. Jiang P, Li J, Han F, et al. Antibiofilm activity of an exopolysaccharide from marine bacterium Vibrio sp. QY101. *PLoS One*. 2011;6(4). doi:10.1371/journal.pone.0018514
71. Akhil K, Jayakumar J, Gayathri G, Khan SS. Effect of various capping agents on photocatalytic, antibacterial and antibiofilm activities of ZnO nanoparticles. *J Photochem Photobiol B Biol*. 2016;160:32–42. doi:10.1016/j.jphotobiol.2016.03.015
72. Saleem S, Ahmed B, Khan MS, Al-Shaeri M, Musarrat J. Inhibition of growth and biofilm formation of clinical bacterial isolates by NiO nanoparticles synthesized from Eucalyptus globulus plants. *Microb Pathog*. 2017;111:375–387. doi:10.1016/j.micpath.2017.09.019
73. He F, Yang Y, Yang G, Yu L. Studies on antibacterial activity and antibacterial mechanism of a novel polysaccharide from Streptomyces virginia H03. *Food Control*. 2010. doi:10.1016/j.foodcont.2010.02.013
74. Xing K, Chen XG, Kong M, Liu CS, Cha DS, Park HJ. Effect of oleoyl-chitosan nanoparticles as a novel antibacterial dispersion system on viability, membrane permeability and cell morphology of Escherichia coli and Staphylococcus aureus. *Carbohydr Polym*. 2009. doi:10.1016/j.carbpol.2008.09.016
75. Mansouri S, Cuie Y, Winnik F, et al. Characterization of folate-chitosan-DNA nanoparticles for gene therapy. *Biomaterials*. 2006;27(9):2060–2065. doi:10.1016/J.BIOMATERIALS.2005.09.020
76. Patil S, Sandberg A, Heckert E, Self W, Seal S. Protein adsorption and cellular uptake of cerium oxide nanoparticles as a function of zeta potential. *Biomaterials*. 2007;28(31):4600–4607. doi:10.1016/J.BIOMATERIALS.2007.07.029
77. Klaassen CD. *Casarett and Doull's Toxicology - The Basic Science of Poisons*. Vol. 12. New York: McGraw-Hill;2008. doi:10.1036/0071470514
78. Lu X, Chunhua L, Xiaoniao C, Zhuo Y. Zinc oxide nanoparticles induce renal toxicity through reactive oxygen species. *Food Chem Toxicol*. 2016;90:76–83. doi:10.1016/j.fct.2016.02.002
79. Sudhasree S, Shakila Banu A, Brindha P, Kurian GA. Synthesis of nickel nanoparticles by chemical and green route and their comarison in respect to biological effect and toxicity. *Toxicol Environ Chem*. 2014;96(5):743–754. doi:10.1080/02772248.2014.923148
80. Zemlyanova MA, Akafeva TI, Dovbysh AA, Smirnov SA. Studies and comparative evaluation of the functional and material cumulation of nano and microdisperse nickel oxide consumed by the peroral route. *Heal Risk Anal*. 2015;(4):36–43. doi:10.21668/health.risk/2015.4.05.eng
81. Kovrižnych JA, Sotníková R, Zeljenková D, Rollerová E, Szabová E. Long-term (30 days) toxicity of NiO nanoparticles for adult zebrafish Danio rerio. *Interdiscip Toxicol*. 2014. doi:10.2478/intox-2014-0004
82. Patra P, Mitra S, Debnath N, Goswami A. Biochemical-, biophysical-, and microarray-based antifungal evaluation of the buffer-mediated synthesized nano zinc oxide: an in vivo and in vitro toxicity study. *Langmuir*. 2012. doi:10.1021/la304120k
83. Seok SH, Cho WS, Park JS, et al. Rat pancreatitis produced by 13-week administration of zinc oxide nanoparticles: biopersistence of nanoparticles and possible solutions. *J Appl Toxicol*. 2013. doi:10.1002/jat.2862